Inhibition effects of a new syntheses aniline derivative on the corrosion of carbon steel in hydrochloric acid solution

A. Saady[1], E. Ech-chihbi[1,2], Z. Rais[1], M. Filali Baba[1], R. Allali[1], K.Cherrak[3], F. EL Hajjaji[1*], B. Hammouti[3], H. Elmsellem[3] and M. Taleb[1]

[1]Laboratoire d'Ingénierie d'Electrochimie, Modélisation et d'Environnement (LIEME), Faculté des sciences/Université Sidi Mohammed Ben Abdellah, Fès, Maroc
[2]Laboratoire des Procédés de Séparation, Faculté des Sciences, Kenitra (LPS), Université IbnoTofail Maroc
[3]Laboratoire de chimie analytique appliquée, matériaux et environnement (LC2AME), Faculté des Sciences, B.P. 717, 60000 Oujda, Morocco

_____

ABSTRACT

The corrosion inhibition of mild steel in molar hydrochloric acid solution by: N1-(2-nitrophenyl)ethane-1,2-diamine (M1) and N1-(2-nitrophenyl)propane-1,3-diamine(M2) has been investigated using gravimetric, potentiodynamic polarization (PP) and electrochemical impedance spectroscopy (EIS) measurements. The influences of inhibitor concentration and solution temperature were investigated. The percentage inhibition efficiency, IE% increased for increasing concentrations and achieved for M1 and M2 96.18% and 94.91% respectively for $10^{-3}M$ at 298K. The associated activation energy of corrosion process and standard free adsorption energies have been determined. These compounds were adsorbed on the mild steel surface according to Langmuir isotherm adsorption model. Some thermodynamic functions of adsorption and dissolution process were calculated and discussed.

Keywords: Mild steel, Aniline, efficiency, Acid inhibition.
_____

INTRODUCTION

Organic and inorganic compounds are widely used as corrosion inhibitors to control the corrosion. Corrosion of mild steel is very importance especially used for structural applications, but it has high rate of dissolution in acidic solution [1-7]Acidic solutions are used extensively in chemical and several industrial processes such as acid pickling, acid cleaning, acid descaling and oil wet cleaning and etc.[1]. The use of inhibitors is one the most practical methods for the protection of metals in acidic medias. These compounds can adsorb on the metal surface and block the active sites and thereby slow down the corrosion rate. The mechanism action of inhibitors is of great importance and depends on the formulation as well as rational use in various environments [8]. Therefore, selecting the appropriate inhibitor for a particular metal is very important. Most of the well-known inhibitors are organic compounds containing nitrogen [9], oxygen [10-11] or food extracts[12].

Cox et al. [13] studied the inhibitory effect of certain aniline derivatives on corrosion of steel in HCl. They showed that a high electron density turn of the nitrogen increases the corrosion potential of these compounds. As for Kaeshe Hackman [14] used some aniline and alkyl amine for delaying the electrochemical kinetics of the process of corrosion of iron.

The aim of the present study was to evaluate the corrosion inhibition efficiency and analyses the inhibitive mechanism of mild steel corrosion in hydrochloric acid by two newly synthesized benzodiazepine compounds; namely, **N1-(2-nitrophenyl)ethane-1,2-diamine**, **N1-(2-nitrophenyl)propane-1,3-diamine** and denoted hereafter

_____

M1 and **M2**, respectively. The study was done using several weightless and electrochemical techniques such as ac impedance measurements and polarization curves. Determination of several parameters related to kinetic activation and the adsorption process may be a tool to ascertain the adsorption mechanism of the inhibitor ion. To this end, correlation between the thermodynamic parameters and the adsorption mechanism was also studied and discussed. The molecular formula of aniline derivatives used in this study is shown in Figure 1.

Figure 1.Molecular structures, names and abbreviations of the studied aniline compounds

N^1-(2-nitrophenyl)ethane-1,2-diamine	N^1-(2-nitrophenyl)propane-1,3-diamine
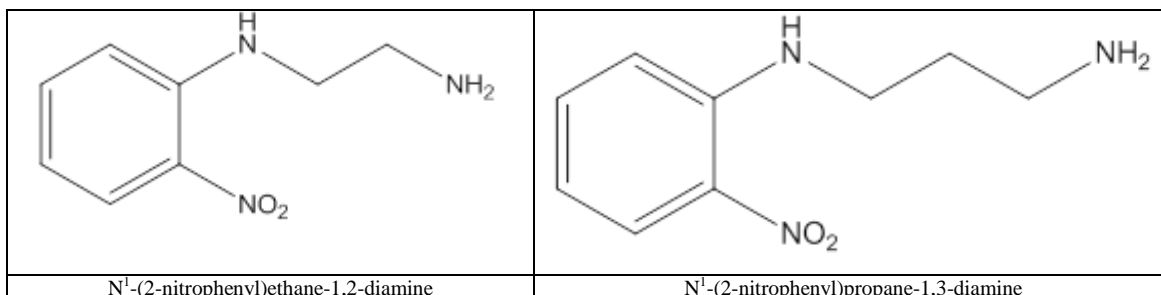
MATERIALS AND METHODS

2.1. Materials preparation
The carbon steel plates (area of 1.0 cm2) with the following composition (weight %): 0.09% P; 0.38% Si; 0.01% Al; 0.05% Mn; 0.21% C; 0.05% S and remainder iron. The surface of specimens was carried out by grinding with emery paper of different grit sizes (from 180 to 1200). The specimens are washed thoroughly with distilled water, degreased and dried with ethanol before use.

2.2. Solutions preparation
The aggressive solution of 1 M HCl was prepared by dilution of analytical grade 37% HCl with doubly distilled water. The solution tests are freshly prepared before each experiment to ensure the reproducibility.

2.3. Weight loss measurements
The weight loss of mild steel in 1 mol.l^{-1} HCl with and without addition of inhibitors was determined after an immersion period in acid for 6 h. After the corrosion test, the specimens were carefully washed in double distilled water, dried and then weighted. Weight loss allowed us to calculate the mean corrosion rate as expressed in mg.cm^{-2}.h^{-1}.

The inhibition efficiency (IE %) was determined by using following Eq. (1) [15]:

$$IE\% = \frac{W_{corr} - W'_{corr}}{W_{corr}} * 100 \qquad (1)$$

Where W_{corr} and W'_{corr} are the values of the corrosion rate in the absence and presence of inhibitor respectively.

2.4. Potentiodynamic measurements
Polarization measurements were performed in a thermally jacketed conventional three-electrode Pyrex cell with a platinum foil counter electrode and saturated calomel electrode (SCE). All measurements were carried out using on an electrochemical measurement system (Volta- Lab 40) comprised of a PGZ 100 potentiostat, a PC and Voltamaster 4 electrochemical software.

The electrode was held in the test environment for 30 min prior to each experiment, which proved sufficient for Ecorr to attain a reliable stable value.

The potential was starting from E_{corr} and moving to a more positive potential or negative potential at a scan rate of 1 mV/s.The linear Tafel segments of anodic and cathodic curves were extrapolated potential to obtain corrosion current densities I_{corr}.

$$IE\% = \frac{I_{corr} - I'_{corr}}{W_{corr}} * 100 \qquad (2)$$

Where I_{corr} and I'_{corr} are the uninhibited and inhibited corrosion current densities respectively.

_____

2.5. Electrochemical impedance measurements

Electrochemical impedance spectroscopy (EIS) was performed using a transfer function analyser (Voltalab PGZ 100), with a small amplitude signal (10 mV rms) over a frequency domain from 100 kHz to 10 mHz at 308 K with five points per decade. Computer programmed automatically and controlled the measurements performed at rest potentials after half an hour of immersion at $E_{corr.}$ The impedance diagrams were given in the Nyquist representation. The impedance diagrams are given in the Nyquist representation. The inhibition efficiency was calculated from charge transfer resistance from the equation (3) [16]:

$$IE\% = \frac{R_{tc/inh} - R_{tc}}{R_{tc/inh}} * 100 \qquad (3)$$

Where $R_{tc/inh}$ and R_{tc} are the charge transfer resistance values with and without inhibitor, respectively.

RESULTS AND DISCUSSION

3.1. Potentiodynamic polarization studies

Polarization curves, obtained in the presence and absence of M1 and M2, after repolarizing the electrode at its E_{corr} for 30mn, are shown in Figure 2.The potential was swept stepwise from the most cathodic potential to the anodic direction.
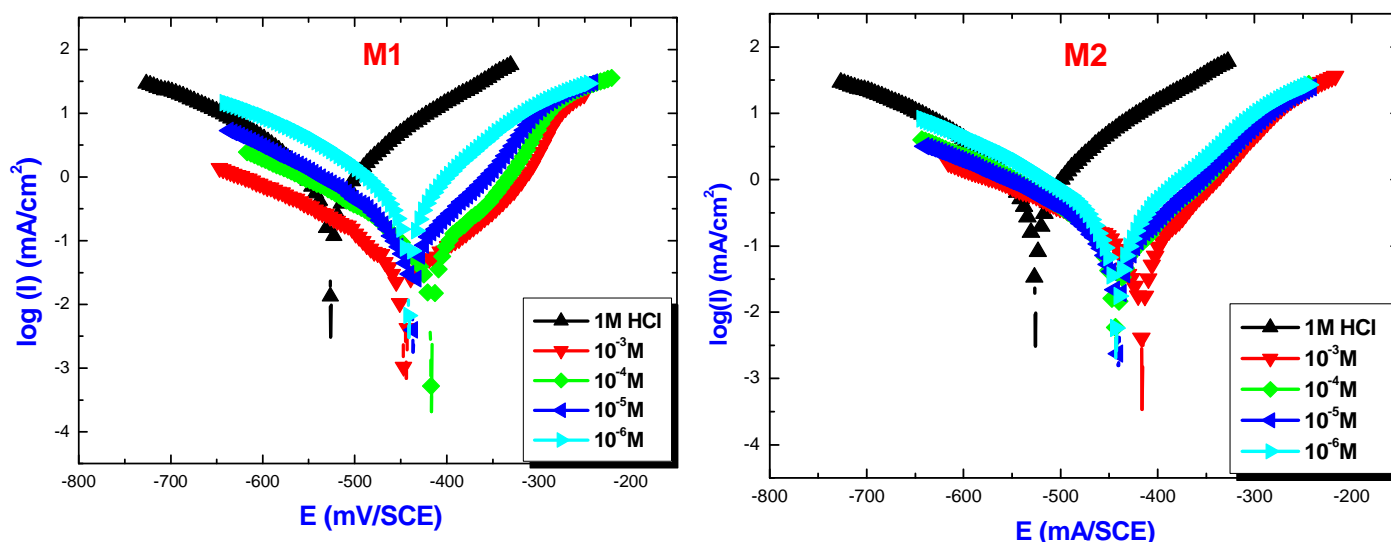
Figure 2. Potentiodynamic polarization parameters of the stainless steel in HCl solution without and with addition of various inhibitors

Table 1.Potentiodynamic polarization parameters of the stainless steel in HCl solution without and with addition of M1 and M2 at 298K

Inhibitor	Concentration (M)	E_{corr} (mV/SCE)	- βc (mV.dec^{-1})	Ba (mV.dec^{-1})	I_{corr} (µA /cm^2)	R_p (ohm /cm^2)	IE (%)
1M HCl	--	-406,8	130,3	-158,8	1830,2	30,14	--
M1	10^{-3}	-544,3	70,9	-57,2	128	204,99	**93,00**
	10^{-4}	-463,7	96,5	-147,5	182,1	431,19	90,05
	10^{-5}	-436,1	80,5	-144,7	216,2	166,62	88,18
	10^{-6}	-441,4	114,5	-151,5	819,1	54,83	55,24
M2	10^{-3}	-414,8	96,6	170,4	151,7	376,83	**91,71**
	10^{-4}	-442,7	90,6	-154,2	218,4	265,55	88,06
	10^{-5}	-441	94,4	-171,5	224,7	219,56	87,72
	10^{-6}	-442,5	101,4	-146,1	378,5	146,70	79,31

From these results we can conclude that the addition of M1 and M2 compounds decreases markedly current density on the cathodic branch whereas little decrease is registered in the anodic branch and the decrease is more pronounced with the increase of the inhibitor concentrations. The slopes of the Tafel line decreases indicating that the inhibition effect is caused by adsorbed inhibiting species [17-21]. These results suggest that these inhibitors mainly act as mixed-type inhibitors with marked cathodic behaviour.

_____

The potential was swept stepwise from the most cathodic potential to the anodic direction; this avoided electrolyte pollution by dissolved iron. Table 1 exemplifies the values of the associated electrochemical parameters: corrosion potentials (E_{corr}), cathodic Tafel slopes (β_c), corrosion current densities (I_{corr}) and inhibiting efficiencies (IE %).

From Table 1.The values of I_{corr} decrease with the rise of M1 and M2 concentrations. We note that the corrosion current densities were significantly reduced in the presence of these compounds and became only 128and 151,7µA/cm^{2}at 10^{-3} M. The higher efficiency obtained is 93 and 91.71% at 10^{-3}M of M1 and M2 successively. This increase in inhibition efficiency with increasing inhibitor concentration may be attributed to the formation of a barrier film, which prevents the attack of acid on the metal surface [22].

3.2. Electrochemical impedance spectroscopy (EIS)
To confirm the obtained results by potentiodynamic polarization curves, and study the inhibition mechanism in more detail, the effects of aniline compounds concentrations on the impedance behaviour of mild steel in 1M HCl solution have been studied. Impedance diagram was plotted to obtain more details on the mechanism of the inhibitor action (Figure 3). The Nyquist plot obtained in the absence and in the presence of the inhibitor showed a semi-circle corresponding to a phenomenon of charge transfer
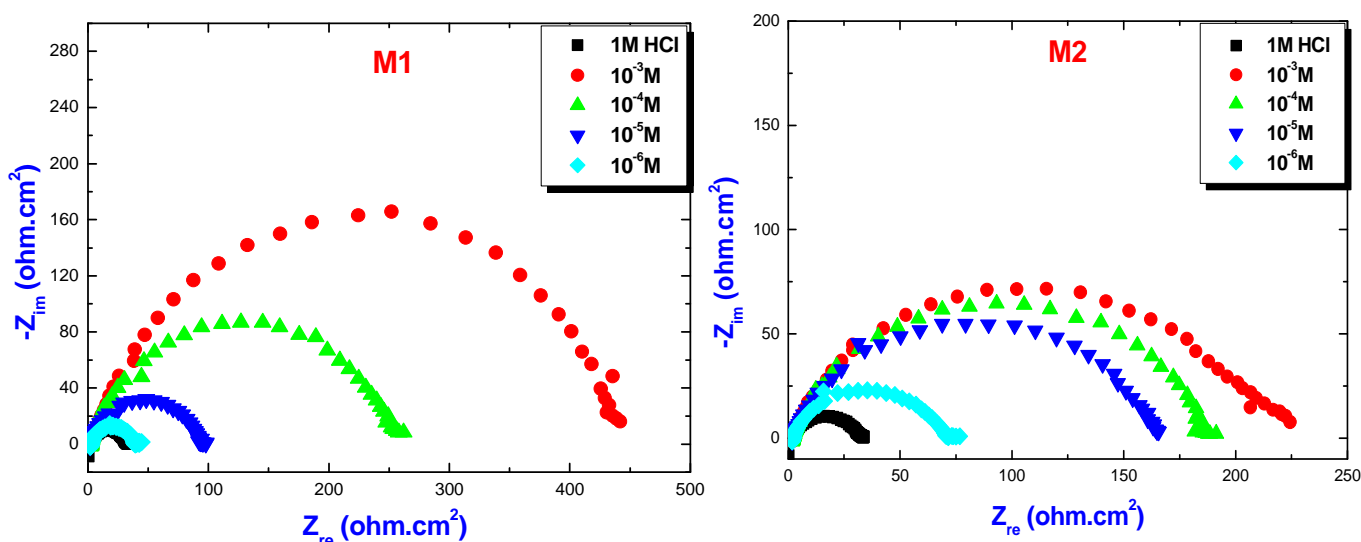
Figure 3. Impedance plot of mild steel obtained in 1M HCl in the absence and presence of various concentrations of inhibitors
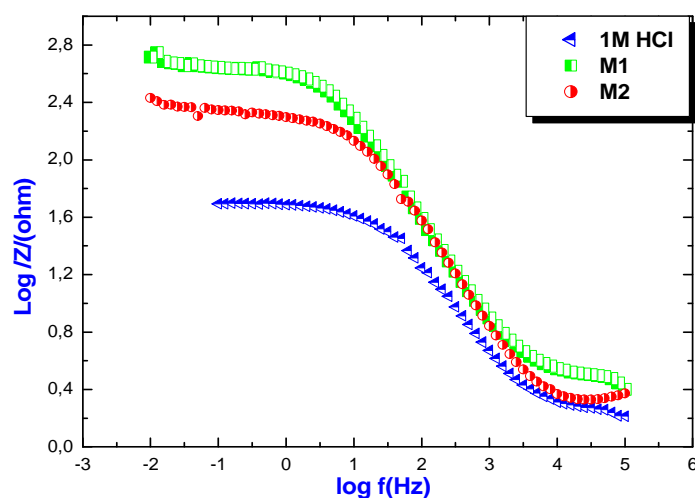
Figure 4. Bode diagrams for carbon steel in 1M HCl, obtained at 298 K without and with addition of the inhibitors at concentrations 10^{-3}M

_____

Nyquist representation of carbon steel in molar hydrochloric acid in absence and presence at different concentrations of CE were presented in Figure 4. The existence of single semi-circle showed the single charge transfer process during dissolution which is unaffected by the presence of inhibitor molecules. Deviations of perfect circular shape are often referred to th1e frequency dispersion of interfacial impedance which arises due to the roughness and other inhomogeneity of the surface [23-24].

The bode diagrams and phase angle curves for carbon steel in 1M HCl without and with various concentrations of these inhibitors are displayed in Figure 4. Inhibition performance is notable according to the impedance values in the low frequency range and the increasing absolute impedance values demonstrate the high inhibition efficiency.

Various parameters summaries the characteristic kinetic parameters associated to the impedance study such as polarization such as resistance (R_{tc}), double layer capacitance Cdl and percentage inhibition efficiency (IE %) have been calculated and listed in Table 2. The polarization resistance values have been calculated from the difference in impedance at higher and lower frequencies [25]. The values of Cdl were obtained at f_{max} using the following equation (4):

$$C_{dl} = \frac{1}{\omega R_{ct}} \quad \text{Where} \quad \omega = 2\pi f_{max} \qquad (4)$$

Table 2.Impedance parameters of mild steel in 1M HCl containing different concentrations of the studied compounds

	Concentration (M)	R_{tc} ($\Omega.cm^2$)	f_{max} (Hz)	C_d ($\mu F/cm^2$)	IE (%)
1M HCl	1	41,04	15,38	312,8	-
M1	10^{-3}	463,856	4,96	68,11	**91,15**
	10^{-4}	238,776	7,90	73,30	82,81
	10^{-5}	101,028	12,24	127,6	59,37
	10^{-6}	44,6046	29,89	131,9	07,99
M2	10^{-3}	241,547	9,96	68,73	**83,00**
	10^{-4}	187,716	9,90	84,47	78,13
	10^{-5}	174,414	9,91	93,37	76,46
	10^{-6}	73,7091	15,43	139,1	44,32

As seen from Table 2, the Rct values of inhibited substrates are increased with the concentration of inhibitors. On the other hand, the values of C_{dl} are decreased with increase in inhibitor concentration which is most probably is due to the decrease in local dielectric constant and / or increase in thickness of the electrical double layer, suggests that CE act via adsorption at the metal / solution interface [26-27].

The impedance of the Nyquist plots were analyzed by fitting the experimental data to a simple equivalent circuit model is given in Figure 5. Which includes the solution resistance R_s and the double layer capacitance C_{dl} which is placed in parallel to the charge transfer resistance R_{ct}.
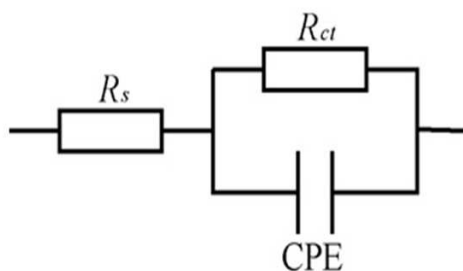
Figure 5. The equivalent circuit model used to fit the experimental EIS data

3.3. Gravimetric measurements
3.3.1. Thermodynamic parameters of the adsorption process
Table 3 regroups the results of weight loss of steel in 1M HCl with and without the addition of various concentrations of the inhibitors studies.

_____

Table 3.Effect of aniline concentration on corrosion of steel in 1M HCl

Inhibitor	Concentration (M)	W_{corr} (mg.cm^{-2}.h^{-1})	IE (%)	Θ
1M HCl	00	0.4821	-	-
M1	10^{-6}	0.2828	41,34	0,413
	10^{-5}	0.1457	69,78	0,697
	10^{-4}	0.0311	93,55	0,935
	10^{-3}	0.0184	**96,18**	0,961
M2	10^{-6}	0.0562	88,34	0,883
	10^{-5}	0.0480	90	0,900
	10^{-4}	0.0227	90,58	0,905
	10^{-3}	0.0245	**94,91**	0,949

The corrosion rate values decrease when the inhibitor percentage increases due to the increase of the inhibition efficiencies. The maximum %IE for each substance was achieved at 10^{-3}M and any further increase in concentration did not cause any appreciable change in the performance of the studied inhibitors. The inhibiting efficiency increases to reach circa 94,91% for M2 and   96,18% at 10^{-3}M in 298K.

Adsorption isotherms are very important in determining the mechanism of organic electrochemical reactions

The adsorption isotherm can be determined if the inhibitor effect is due mainly to the adsorption on metallic surface. The adsorption isotherm type can provide additional information about the tested compounds properties. The fractional coverage surface (θ) easily determined from weigh loss by the ratio E%/100. The values of IE% do no differ substantially from θ as shown in Table 3.

Several adsorption isotherms were assessed. The best fitted straight line (Fig. 3) is obtained from the plot of C$_{inh}$/**θ** versus C$_{inh}$ with nearly unitslope(>0,999)and the best fits are obtained with Langmuir's adsorption isotherm as given in the equation 5:

$$C_{inh}/ \; \theta = 1/ \; K_{ads} + C_{inh} \quad (5)$$

Where C$_{inh}$ is the inhibitor concentration and K$_{ads}$ is the equilibrium constant for the adsorption process.

The free adsorption energy is calculated from the equilibrium adsorption constant is given in the equation 6:

$$\Delta G^{0}_{ads}= -RT \; ln55.5 \; K_{ads} \quad (6)$$

55.55 represents the concentration of water in solution in mol L-1, **R** is the universal gas constant and **T** is the absolute temperature.
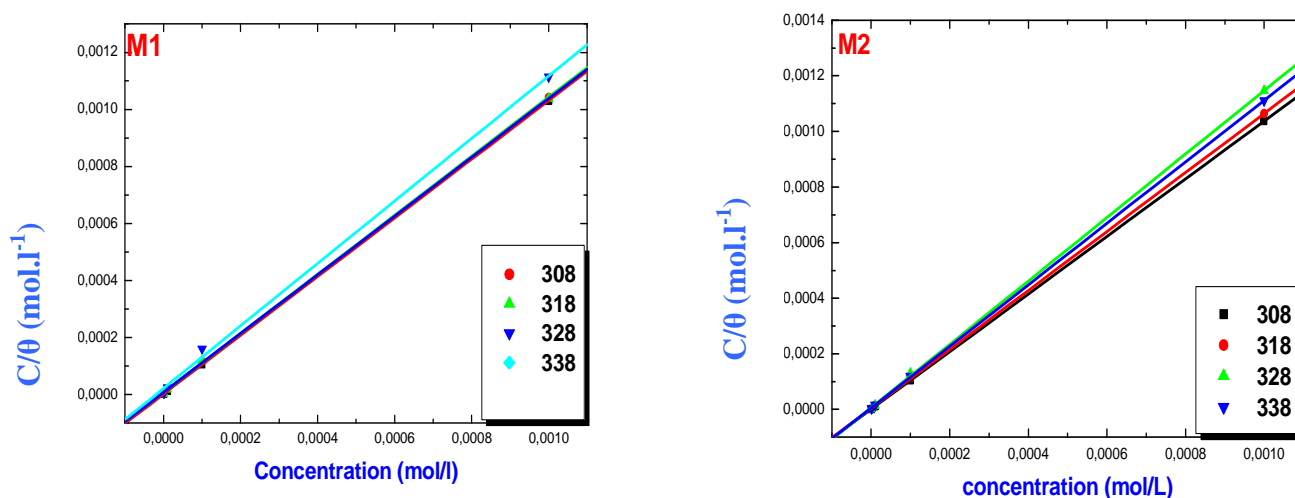
Figure 6. Langmuir isotherm adsorption model on the steel surface M1 and M2 in 1 M HCl

The plots of Figure 6 reflecting the evolution C$_{inh}$/θ versus C$_{inh}$are with slope around unity which suggests that these compounds adsorbs on the metal surface obeying to the Langmuir's adsorption isotherm. The thermodynamics

_____

parameters derived from Langmuir adsorption isotherms for the studied compounds, are given in Table 4. The standard free energy of adsorption values of -20 kJ mol^{-1}or less negative are associated with an electrostatic interaction between charged molecules and charged metal surface physisorption, those of -40 kJ mol^{-1} or more negative involve charge sharing or transfer from the inhibitor molecules to the metal surface to form a coordinate covalent bond, chemisorption [28-29].

Resulted in terms of $\Delta G°ads$ equal to **-41,48kJ mol^{-1}**for M1 and **-45,30kJ mol^{-1}**at 338 K (Table 4) in the range of studied temperatures. The low and negative values of $\Delta G°ads$ indicate the spontaneous adsorption of inhibitors on the mild steel surface. This kind of isotherm, generally regarded to indicate chemisorption.

The thermodynamic parameters $\Delta H°_{ads}$and $\Delta S°_{ads}$for the adsorption of the studied inhibitors on mild steel are calculated from the two equations:

- **Van't Hoff** [30]: $$K = \frac{1}{55,5}\exp\left(\frac{-\Delta G°_{ads}}{RT}\right) \qquad (7)$$

- **Gibbs–Helmholtz** [31]: $\Delta G°ads = \Delta H°ads - T\Delta S°ads.$ **(8)**

The negative values of $\Delta H°_{ads}$mean that the dissolution process is an exothermic phenomenon. It assumed that an exothermic process is attributed to either physical or chemical adsorption but endothermic process corresponds solely to chemisorption. The positive values of $\Delta S°_{ads}$ is generally explained a disordered of adsorbed molecules of inhibitor with the progress in the adsorption onto the mild steel surface [32-33].

Table 4. Thermodynamic parameters for the adsorption of M1 and M2 on C38 steel at different temperatures

Inhibitor	Temperature (K)	K_{ads}	$\Delta G°_{ads}$ (KJ/mol)	$\Delta H°_{ads}$ (KJ/mol)	$\Delta S°_{ads}$ (KJ/mol)
M1	308	$2,17.10^6$	-47,62	-47,16	20,32
	318	$1,30.10^5$	-41,73		
	328	$1,26.10^5$	-42,95		
	338	$4,67.10^4$	-41,48		
M2	308	$3,71.10^6$	-48,99	-30,20	47,87
	318	$2,74.10^5$	-43,70		
	328	$1,65.10^5$	-43,70		
	338	$1,82.10^5$	-45,30		
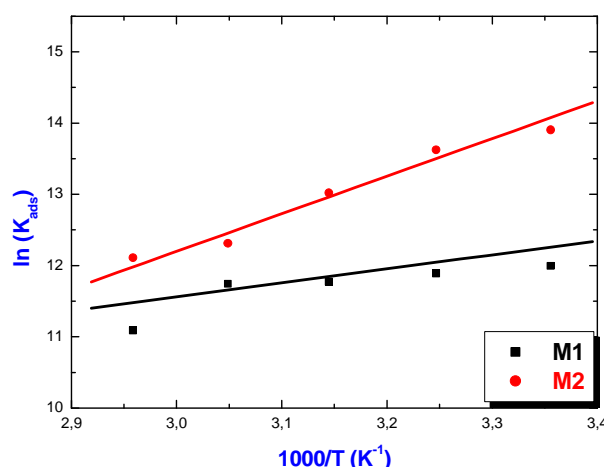
Figure7. The linear dependence with LnK$_{ads}$ versus 1000/T

3.3.2. Kinetic parameters of activation
The temperature can modify the interaction between the mild steel and the acidic solution in the absence and in the presence of inhibitors. Weight loss measurements for mild steel in 1 M HCl at different concentrations of the M1 and M2, in the temperature range 318–338 K, during a period of 2 hours are shown in Table 5.

_____

Table 5. Influence of temperature on the corrosion rate of mild steel in the presence and absence of inhibitors M1 and M2 at various concentrations for 2h immersion time

Temperature (K)	Concentration (M)	M1		M2	
		W_{corr} (mg cm^{-2} h^{-1})	IE (%)	W_{corr} (mg cm^{-2} h^{-1})	W_{corr} (mg cm^{-2} h^{-1})
308	00	1,9695	-	1,9695	-
	10^{-3}	0.0588	**97,00**	0.0699	**96,4**
	10^{-4}	0,1015	94,84	0,0656	96,6
	10^{-5}	0,3013	84,70	0,1835	90,6
	10^{-6}	0,6768	65,63	0,4941	74,9
318	00	1,69075	-	1,69075	-
	10^{-3}	0.0691	**95,91**	0.1004	**94,0**
	10^{-4}	0,2437	85,58	0,1918	88,6
	10^{-5}	0,8020	52,56	0,4908	70,9
	10^{-6}	1,0317	38,98	0,8756	48,2
328	00	2,8338	-	2,8338	-
	10^{-3}	0.1049	**96,38**	0.3598	**87,3**
	10^{-4}	0,4397	84,48	0,6368	77,5
	10^{-5}	1,2483	55,95	0,8954	68,4
	10^{-6}	1,7625	37,84	1,4137	50,1
338	00	4,07715	-	4,07715	-
	10^{-3}	0.4189	**89,72**	0.4047	**90**
	10^{-4}	1,5328	62,40	0,6823	83,2
	10^{-5}	2,3495	42,37	1,6060	60,6
	10^{-6}	3,2280	20,82	2,7215	33,2
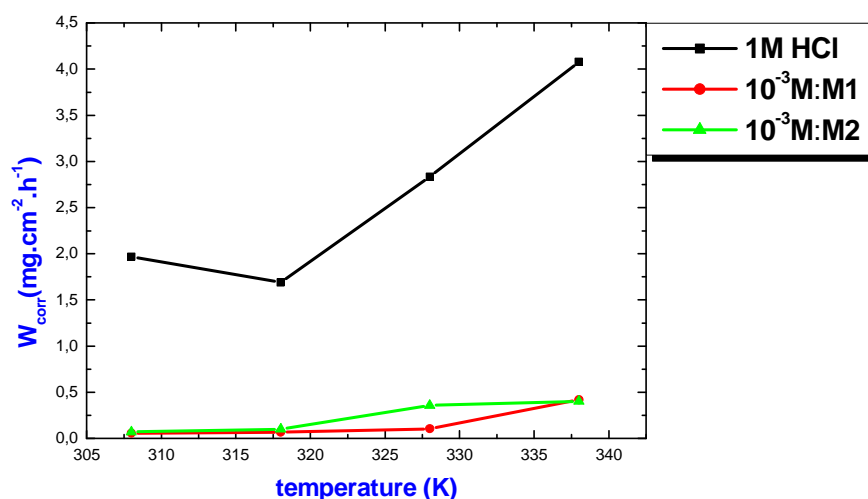
Figure 7. Variation of corrosion rate with temperature for mild steel in 1 M HCl in the presence of 10^{-3}M of M1 and M2

It is clear from Figure **7** and Table 6 that the increase of corrosion rate is more pronounced with the rise of temperature for blank solution. Also, the inhibition efficiencies decrease slightly with increasing of temperature indicating that higher temperature dissolution of steel predominates on adsorption of inhibitors studies at the metal.

To calculate activation thermodynamic parameters at different concentrations of these compounds such as activation energy E_a, entropy $\Delta S°$ and enthalpy $\Delta H°$ of activation, Arrhenius Eq. (9) and its alternative formulation called transition state Eq. (10) were used:

$$\text{Wcorr} = A e^{\left(\frac{-Ea}{RT}\right)} \qquad (9)$$

$$W = \frac{RT}{Nh} \exp\left(\frac{\Delta S^*}{R}\right) \exp\left(-\frac{\Delta H^*}{RT}\right) \qquad (10)$$

T is the absolute temperature, K is a constant and R is the universal gas constant, h is plank's constant, N is Avogadro's number.

The activation energy E_a is calculated from the slope of the plots of Log (W_{corr}) vs. 1/T (Figure 8). Plots of Log(W_{corr}/T) vs. 1000/T give a straight line with a slope of $\Delta H°$/R and an intercept of (Log(R/Nh)+ $\Delta S°$/R) as shown in Fig.

_____

10. From this relation the values of ΔH° and ΔS° can be calculated. The calculated parameters at different concentrations of the inhibitor are collected in Table 6.
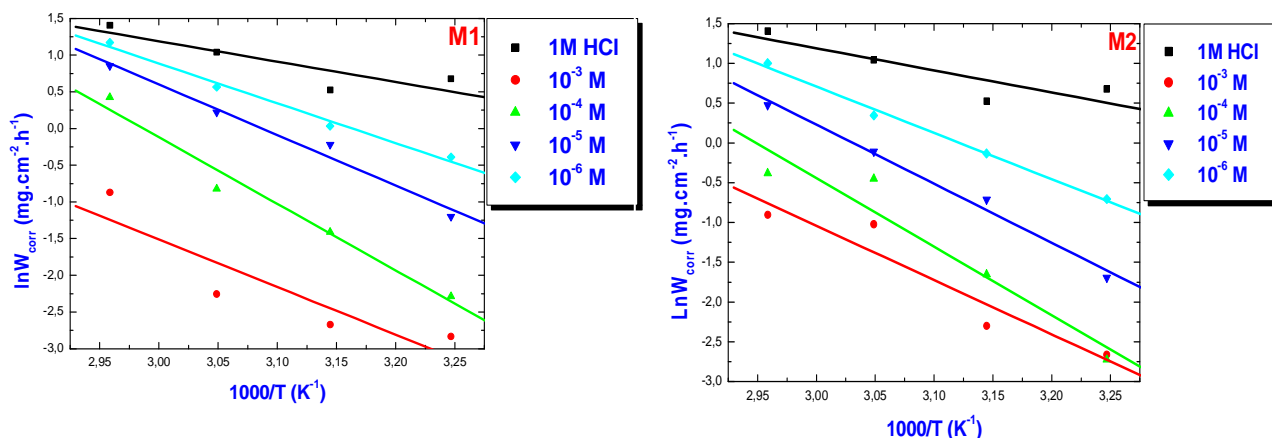
Figure 8. Arrhenius plots of mild steel in 1 M HCl at different concentrations of M1 and M2

Table 6. Activation parameters Ea, ΔH* and ΔS* of mild steel dissolution in 1 M HCl in the absence and in the presence of M1 and M2 at different concentrations

Concentration (M)	Ea (kJ mol-1)		ΔH* (kJ mol-1)		ΔS* (J K-1 mol-1)	
--	23,08		20 ,40		-174,91	
10⁻³	53,17	55,95	50,99	54,09	-105,7	-92,41
10⁻⁴	74,32	70,70	72,73	69,05	-28,81	-42,53
10⁻⁵	56,53	60,86	54,67	59,07	-76,99	-66,89
10⁻⁶	44,45	47,71	42,42	45,73	-111,37	-102,94

The lower value of *Ea* in inhibited solution when compared to that for uninhibited one shows that strong chemisorption bond between the inhibitor and the metal is highly probable. In the opposite case a physisorption can usually occur. From Table 6, it appears that the activation energy values obtained are 43.24 and 91.03 kJ/mol in inhibited (10⁻³M of M1 and M2) and uninhibited solutions, respectively. It is clear that the activation energy increases in presence of the inhibitor. Generally, the inhibitive additives cause a rise in activation energy value when compared to the blank. Popova et al. [34] pointed out that the decrease of inhibition efficiencies may be attributed to the specific interaction between the iron surface and the inhibitor components. The higher value of activation energy of the corrosion process, in the presence of M1 and M2, is attributed to an electrostatic adsorption mechanism of the inhibitor [34-36].
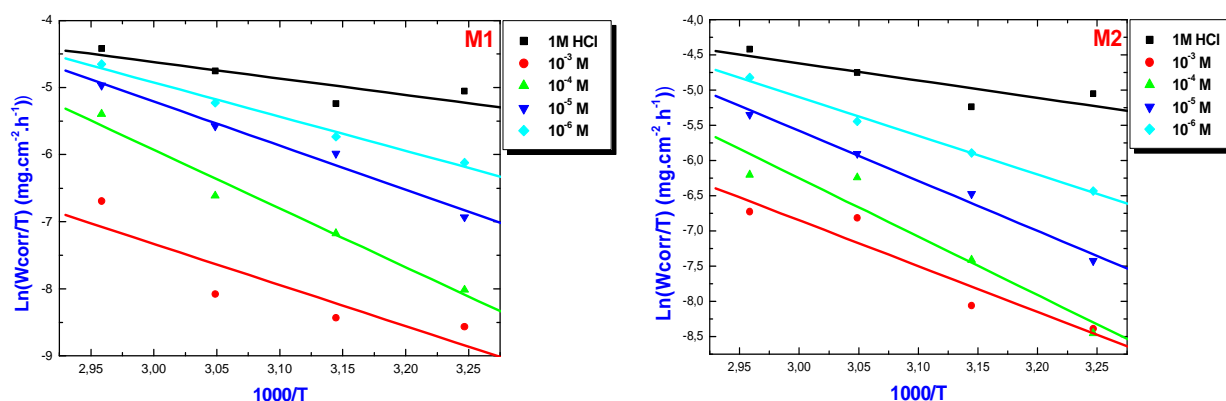
Figure 9. Arrhenius plots of lnW_corr/T versus 1000/T at different concentrations of M1 and M2

The positive signs of ΔH* reflecting the endothermic nature of the steel dissolution process. It is obviously that the activation energy strongly increases in the presence of the inhibitor. Some authors [31-32] have attributed this result to the inhibitor species being physically adsorbed on the metal surface. The entropy of activation ΔS* in the absence

_____

of inhibitors is positive and this value increases positively with the inhibitor concentration, this increase of implies that an increase in disordering takes place on going from reactants to the activated complex [37].

3.4. Scanning Electron Microscopy (SEM)

The Figures 11and 12 represent the scanning electron microscopic (SEM) images of mild steel surface in 1M HCl solution without and with inhibitors of mild steel that has been exposed to the 1M HCl for 6h in the absence and presence of studied inhibitors, respectively.

Figure 10: SEM image of mild steel surface (a) before immersion in 1M HCl, (b) after 6 hours of immersion in 1M HCl solution in the absence of inhibitors
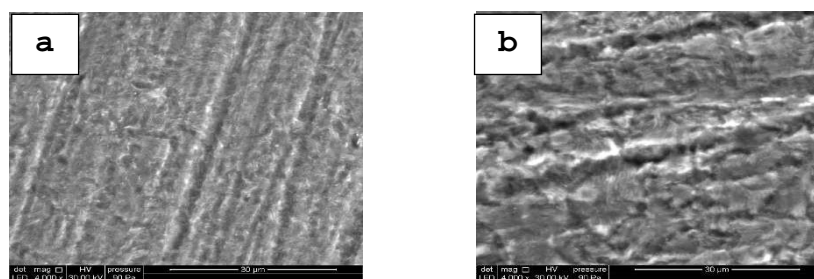
Figure 11: SEM image (x30μm) of mild steel after 6 hours of immersion in 1M HCl solution with 10^{-3} M of inhibitor M1(a) and M2 (b)

The SEM images show that the surface of carbon steel is highly damaged in the uninhibited solution (Figure 10) However, a smoother surface is seen in the presence of the inhibitor (Figure 11). These results indicate that the inhibitor molecules hinder the dissolution of carbon steel by formation of a protective film on the steel surface.

CONCLUSION

● The studied benzodiazepine compounds show good inhibition properties for mild steel corrosion in 1 M HCl solutions.

● The inhibition efficiency of the studied inhibitors increased with inhibitor concentrations.

● Potentiodynamic polarization measurements of M1 and M2 indicate that the studied inhibitors act predominantly as mixte-type inhibitors which retarding both the cathodic process without changing the mechanism of corrosion process.

REFERENCES

[1] S. EL Arouji, K. AlaouiIsmaili, A. Zerrouki, S. El Kadiri, Z. Rais, M. Filali Baba, M. Taleb, Khadijah M. Emran, A. Zarrouk, A. Aouniti and B. Hammouti, *Der Pharma Chemica,* **2015***, 7(10),67-76.

[2] H. Elmsellem, N. Basbas, A. Chetouani, A. Aouniti, S. Radi, M. Messali, B. Hammouti, *Portugaliae. Electrochimica. Acta*, **2014**, 2, 77.

[3] D. Ben Hmamou, R. Salghi, A. Zarrouk, M. Messali, H. Zarrok, M. Errami, B. Hammouti, Lh. Bazzi , A. Chakir, *Der Pharm. Chem*, **2012**, 4, 1496.

[4] A. Ghazoui, N. Bencaht, S.S. Al-Deyab, A. Zarrouk, B. Hammouti, M. Ramdani, M. Guenbour, *Int. J. Electrochem. Sci*, **2013**, 8, 2272.

[5] A. Zarrouk, H. Zarrok, R. Salghi, N. Bouroumane, B. Hammouti, S.S. Al-Deyab, R. Touzani, *Int. J. Electrochem. S*ci, **2012**, 7, 10215.

[6] H. Elmsellem, K. Karrouchi, A. Aouniti, B. Hammouti, S. Radi, J. Taoufik, M. Ansar, M. Dahmani, H. Steli, B. El Mahi, *Der Pharma Chemica*, **2015**, 7(10), 237-245.

[7] S. Rekkab, H. Zarrok, R. Salghi, A. Zarrouk, Lh. Bazzi, B. Hammouti, Z. Kabouche, R. Touzani, M. Zougagh, *J. Mater. Environ. Sci*., **2012**, 3, 613

_____

[8] S. El Arrouji, K. Ismaily Alaoui, A. Zerrouki, S. EL Kadiri, R. Touzani, Z. Rais,M. Filali Baba, M. Taleb, F. El-Hajjaji, A. Chetouani, A. Aouniti, *J. Mater. Environ. Sci.* **2016**, 7 (1), 299-309.

[9] Y. Jianguo, W. Lin, V. Otteno-Alegoi and D.P. Schweinsberg, *Corros.Sci*, **1995**, 37, 975.

[10] F. El-Hajjaji, R.A. Belkhmima, B. Zerga, M. Sfaira, M. Taleb, M. EbnTouhami, B Hammouti. S.S. Al-Deyab, E. Ebenso, *Int. J. Electrochem. Sci*, 9 (**2014**) 4721 – 4731.

[11] L. Afia, R. Salghi, O. Benali, S. Jodeh, I. Warad, E. Ebenso and B. Hammouti, *Portugaliae Electrochim. Acta*, **2015**, 33(3), 137.

[12] L. A. Al Juhaiman, A. A. Mustafa and W. K. Mekhamer, *Anti-Corros*, **2013**, 1, 28.

[13] P.F. Cox, R.L. Every, O.L.Riggs, *Corr*, **1964**, 20, 299

[14] H. Kaesche, N. Hackeman, *J. Electrochem. Soc.*, **1958**, 105, 191

[15] H. Elmsellem, A. Elyoussfi, H. Steli, N. K. Sebbar, E. M. Essassi, M. Dahmani, Y. El Ouadi, A. Aouniti, B. El Mahi, B. Hammouti, *Der Pharma Chemica*, **2016**, 8(1), 248-256.

[16] N. Abdulwali, F. Mohammed, A. Al subari2, H. Ghaddar3, A. Guenbour, A. Bellaouchou, E. arEssassi, Robert A Cottis, *Int. J. Electrochem. Sci*, **2014**, 9, 6402 – 6415.

[17] K. Ismaily Alaoui F. Ouazzani, Y. kandrirodi, A.M. Azaroual, Z. Rais, M. Filali Baba , M. Taleb, A. Chetouani, A. Aouniti, B. Hammouti, *J. Mater. Environ. Sci.* **2016**, 7 (1), 244-258.

[18] M.B. Cisse, B. Zergar, F. El Kalai, M. EbnTouhami, M. Sfaira, M. Taleb, B. Hammouti, N. Benchat, S. El Kadiri, A. Touimi Benjelloun, *Surface Review and Letters,* **2011**, 18, 303.

[19] M.A.M. Ibrahim, M. Messali, Z. Moussa, A.Y. Alzahrani, S.N. Alamry, B. Hammouti, *Portug. Electrochim. Acta,* **2011**, 29, 375.

[20] B. Zerga, B. Hammouti, M. EbnTouhami, R. Touir, M. Taleb, M. Sfaira, M. Bennajeh, I. Forssal, *Int. J. Electrochem. Sci,* 2012, 7, 471.

[21] K. Benbouya, B. Zerga, M. Sfaira, M. Taleb, M. EbnTouhami, B. Hammouti, H. Benzeid, E.M. Essassi, *Int. J. Electrochem. Sci.,* **2012**, 7, 6313

[22] O. Benali, M. Ouazene, *Arab. J. Chem.* **2011**, 4, 443.

[23] J. Aljourani, K. Raeissi, M. A. Golozar, *Corros. Sci*, **2009**, 18, 36.

[24] O. Benali, L. Larabi, M. Traisnel, L. Gengembra, Y. Harek, *Appl. Surf. Sci*, **2007**, 253, 6130.

[25] I. Chakib, H. Elmsellem, N. K. Sebbar, S. Lahmidi, A. Nadeem, E. M. Essassi, Y. Ouzidan, I. Abdel-Rahman, F. Bentiss, B. Hammouti., *J. Mater. Environ. Sci*, **2016**, 7(6), 1866-1881.

[26] M. A. Quraishi, J. Rawat, *Mater. Chem. Phys*, **2001**, 70, 95.

[27] A. Amin Mohammed, S. Abd El-RehimSayed, E. E. F. El-Sherbini, S. BayoumiRady, *Electrochim. Acta*. **2007**, 52, 3588.

[28] O.L.Riggs, R.M.Hurd, *Corrosion,* **1967**, 23, 252.

[29] Juttner K.*, Electrochim. Acta,* **1990**, 35, 1501.

[30] G.K. Jennings, P.E. Laibinis, *Colloids Surf, A,* **1996**, 116, 105

[31] Z. Zhang, S. Chen, Y. Li, *Corros. Sci*, **2009**, 51, 291.

[32] *B. Zerga , B. Hammouti, M. EbnTouhami, R. Touir, M. Taleb, M. Sfaira, M. Bennajeh3, I. Forssal, Int. J. Electrochem. Sci,* **2012**, 7, 471 – 483.

[33] H. Elmsellem, A. Aouniti, M. Khoutoul, A. Chetouani, B. Hammouti, N. Benchat, R. Touzani, M. Elazzouzi, *Journal of Chemical and Pharmaceutical Research*, **2014**, 6(4), 1216-1224.

[34] *L. Afia, R. Salghi1, Eno. E. Ebenso, M. Messali, S. S. Al-Deyab, B. Hammouti, Int. J. Electrochem. Sci,* **2014**, 9, 5479 - 5495

[35] A. Popova, E. Sokolova, S. Raicheva, M. Christov, *Corros. Sci*, **2003**, 45, 33.

[36] H. Elmsellem, H. Nacer, F. Halaimia, A. Aouniti, I. Lakehal, A. Chetouani, S. S. Al-Deyab, I. Warad, R.Touzani, B. Hammouti, *Int. J. Electrochem. Sci*, **2014**, 9, 5328

[37] F. Mounir, S. El Issam1, Lh. Bazzi, O. Jbara, A. ChihabEddine, M. Belkhaouda, L. Bammou, R. Salghi, L. Bazzi, *Mor. J. Chem*, **2014**, 2(1), 33.